CFD investigation of the influence of low emissivity coatings to reduce domestic energy consumption

CFD investigation of the influence of low emissivity coatings to reduce domestic energy consumption

S Buckingham[1], C. Goffaux[1], D Jacquet[2] and L Geron[3]
[1] Energy and Buildings team, Cenaero, Belgium.
[2] ArcelorMittal Montataire Research, France.
[3] ArcelorMittal Liège Research, Belgium.

E-mail: sophia.buckingham@cenaero.be

Abstract. The opportunity to perform energy savings at a kitchen room scale was numerically explored by applying low emissivity coatings to internal surfaces of walls and external casings of appliances. The study focuses on the radiator's heating consumption necessary to maintain the desired comfort temperature. The objective is to provide reliable scientific proof of the added value of low emissivity coatings by performing CFD (Computational Fluid Dynamics) simulations. Based on this domestic cavity model and a gray-body approach, a parametric study was performed covering a wide range of surface emissivity combinations, in winter weather conditions. The risk of overheating is also analyzed in summer weather conditions.

1. Introduction

As a large portion of the unwanted heat flux goes through the envelope of buildings, better understanding the influence of surface properties may significantly contribute to lower these losses. In particular, appropriate optical functions such as solar reflectance and infrared emissivity can be very beneficial.

ArcelorMittal is looking into the benefits of developing low emissivity coatings to reduce domestic energy consumption, and more specifically the heating consumption of a room. More specifically, it is based on technologically advanced products in the form of controlled and optimized emissivity surfaces. The primary objective is to provide reliable scientific proof demonstrating the concept's value and commercial interest, in the form of state-of-the art Computational Fluid Dynamics (CFD) numerical simulation. The strengths of the CFD approach are to provide a 3D-representation of the local flow conditions while allowing for a detailed description of the numerical model. The chosen test case is representative of a kitchen equipped with an oven and a fridge as appliances and a radiator. Multi-physic calculations, coupling the convective, conductive and radiative heat exchanges, are computed. In the absence of experimental validation, a high-fidelity model is developed based on an incremental and comparative approach.

The first task of the project has been to set-up the adequate models and tools to best represent the domestic cavity. Particular care is taken while setting-up the various boundary conditions in order to be consistent with standards effectively used in building physics while delivering representative results. Once these features implemented, the cavity model is exploited by varying the emissivity values of the walls and outside casings of the appliances. The surfaces are regrouped by logical types

and treated as gray-bodies while limiting the emissivity to a standard and low value in order to best characterize the coating's impact. These simulations are performed in both winter and summer weather conditions. These different configurations effectively induce changes in the radiative exchanges in between the various surfaces which directly affects the room's behavior as a whole. Consequently, a set of characteristic thermal outputs are compared based on which the profitable use of the coating in terms of energy savings is demonstrated according to the surface applications.

2. Methodology

2.1. Governing equations and turbulence model

The simulations are performed with the CFD package *ANSYS FLUENT 13.0* [1], which uses the control volume method. Unsteady Reynolds Average Navier-Stokes (URANS) equations are used in combination with the energy equation to account for the thermal effects. Furthermore, the Boussinesq equation is best-suited to represent these thermo-convective effects as the temperature gradient between the external casing, the heated walls and the ambient is acceptable. The pressure-based solver is selected as it is the best-suited to low speed flows. Although the emissivity remains constant in this study, the radiative exchanges are modeled by the DO radiation model, only model able to overcome this gray-body simplification and offer the possibility of defining multiple wavelength bands. This will allow us to compare the effect of the gray-body hypothesis in the continuation of this work. Flow turbulence is modeled and the k-epsilon Realizable turbulence model is chosen for closure. A second order upwind-scheme is used to improve sptatial accuracy and limit diffusivity.

2.2. Kitchen configuration and computational mesh

The selected case is representative of a room which is 4 meters wide in both directions and 2.5 meters high. It is equipped with an oven (0.5x0.5x0.4 meters) placed on a working plane, a fridge close to the (y+) wall and a radiator positioned along the opposite wall. The computational domain comprises the air volume of the room and the 4 cm thick insulation casings of the appliances. A view of the room is proposed on figure 1. All walls are infinitely thin, however their thermal resistance is accounted for by the 'shell conduction' option proposed by *ANSYS FLUENT*.

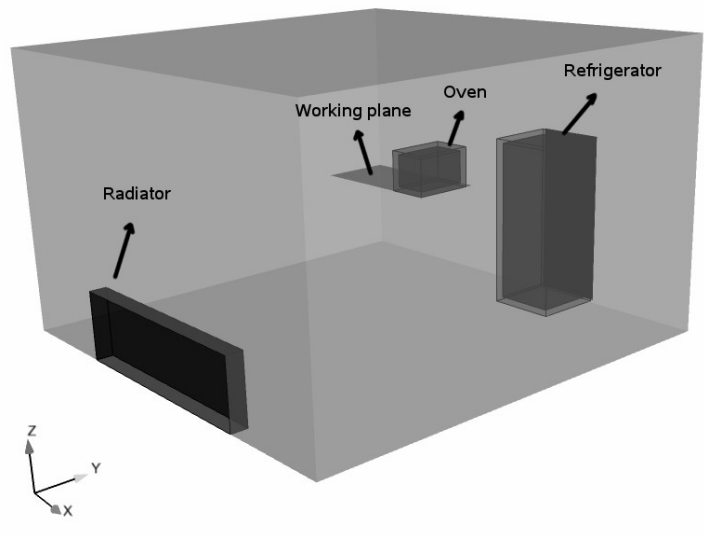

Figure 1. Kitchen configuration

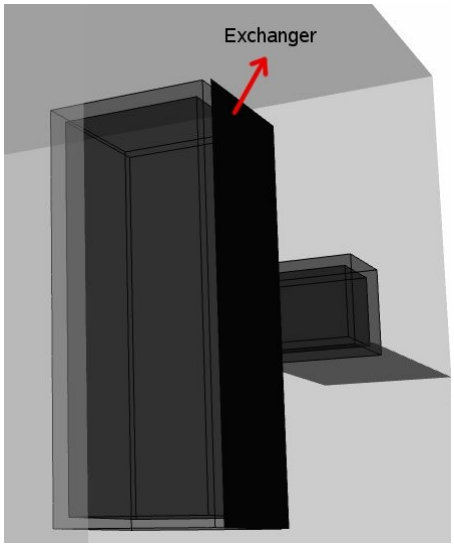

Figure 2. Fridge exchanger

This approach takes into account the conductive exchanges perpendicular to the wall as well as the wall's inertia in case of transient simulations. A fictitious thickness of 15 cm is affected to all walls. Only the (x+) wall is in direct contact with the exterior while all others are in contact with neighboring

rooms. The radiator is modeled by a volume of air that measures 1x0.15x0.5 meters and the front (y+) solid vertical plate. The fridge is represented by its main components illustrated on figure 2 with the exchanger slightly shifted compared to the evaporator placed vertically at the back of the main casing, that measures 0.6x0.6x1.5 meters. Finally, material properties given by the density ρ, the specific heat C_p and the conductivity k are summarized in table 1.

Table 1. Material properties.

Material	Surface	ρ [kg/m^3]	C_p [J/(kg.K)]	k [W/(m/K)]
Concrete	Walls (x-, y±, z±)	1500	840	1.2
Insulation 1	Fridge casing	15	1400	0.02
Insulation 2	Oven casing	15	1400	0.08
Wood	Work plane	700	2310	0.17
Concrete-insulation	Exterior wall (x+)	1005	842	0.11

The properties of the exterior wall (x+) are homogenized by weighting according to the thickness of the individual layers. A relatively coarse mesh was generated with the software *GAMBIT* and used throughout the study in order to keep a reasonable computational time. The 'standard' wall function (SWF) is chosen to approximate the near-wall effects, with a first cell size of 3 cm ($y_{+,max} \sim 45$). The maximum cell size is kept below 25 cm, which results in a total number of 539 845 cells. Moreover, it is likely that the mesh has little influence on the global quantities of interest such as the average temperature of the room, or the average heat fluxes experienced by the appliances. This approach is supported by the fact that the comparative study is carried-out in relative values.

3. Implementation of the CFD simulation

3.1. Boundary conditions

3.1.1. Walls and envelops of appliances. The kitchen walls can be distinguished as follows: the interior walls (x-, y±), the exterior wall (x+) and the horizontal walls (ceiling z+ and ground z-). An "adiabatic" boundary condition (BC) is applied to these last two walls, considered well isolated. A "mixed" type of BC is affected to all vertical walls, allowing to distinguish between convective and radiative heat exchanges with the surroundings. The convective exchanges are characterized by attributing a value to the convective heat transfer coefficient (CHTC) and to the free-stream temperature T_∞. As for the radiative exchanges, these are defined by specifying the external radiation temperature T_{rad} and the internal and external emissivities. The CHTC values are fixed according to ISO standards [2]. In the case of interior walls, the free-stream and external radiative temperatures both correspond to the average temperature present in the neighboring rooms. The internal emissivity is directly equal to the surface's emissivity ε_s but for the external emissivity value the cavity effect must be considered since the neighboring rooms are not being modeled. This effect is simplified to the case of two infinite parallel walls, such that: $\varepsilon_{corr} = 1/[(1/\varepsilon_s)+(1/\varepsilon_s)-1]$.

Naturally, this last point differs for the exterior wall, where radiative exchanges are corrected by a factor F_r=0.5 [2] to take the surface's vertical inclination into account. The low-emissivity coating will not be applied to this outside surface but a standard emissivity value (divided by two) will be applied. The free-stream and external radiative temperatures remain equal to each other to match with 1D-building modeling softwares for future comparison. These both correspond to the exterior temperature T_{ext}. In order to represent extreme weather situations, the average values measured in Stockholm throughout January (at 6:22 am) [10] are chosen to represent winter conditions. All boundary condition values are summarized in table 2. A "convective" type of BC values is applied to the oven

and fridge. An inside temperature of 5 °C is advocated [2, 3] for a fridge and 200 °C represents a typical cooking temperature for an oven. The CHTC values are adjusted by inverse analysis to obtain realistic temperature gradients between the interior walls and inside temperatures of around 4 °C [4] and 45 °C [5, 6] when the fridge and oven are 'on' respectively. These parameters are fixed to 5 W/(m².K) for the oven and 3 W/(m².K) for the fridge. A "constant temperature" BC is affected to the fridge components. The exchanger, positioned at the back of the fridge by simplification [7, 8], is fixed to 50 °C whereas a temperature of -0.5 °C is assigned to the evaporator, taken equal to the average value of the 'on/off' cycles it typically follows [9].

Table 2. Boundary conditions applied to vertical walls (ε_s: surface emissivity)

Wall	T_∞ [°C], T_{rad}	h_c [W/(m².K)]	Internal ε	External ε	$Q_{s\text{-}eff}$ [W/m²]
Interior	20 in winter 23 in summer	2.5	ε_s	$1/[(1/\varepsilon_s)+(1/\varepsilon_s)-1]$	x
Exterior	-1.8 in winter 27.8 in summer	23	ε_s	$\varepsilon_s/2$	0

3.1.1. Radiator. The radiator has been designed to provide 2/3-1/3 proportions between convective and radiative contributions to the room. To respect this ratio, the radiator is modeled in two parts. The vertical plate accounts for both types of exchanges while the source volume is purely convective. A "constant temperature" BC is applied to the plate with a realistic value of 50 °C. As for the heat source, the source is tuned and finally adjusted to 500 W so as to reach a comfort temperature of 23 °C (from an initial temperature of 15 °C) in a realistic time of slightly less than 2 hours, as shown on figure 3. Finally, in order to account for the plate's inertia, ramps of 3 minutes are implemented in between the 'on' and 'off' cycles.

3.2. Time step dependency study

After completing the preparation phase of the model, several sensitivity studies are conducted to optimize the simulation parameters. This is an essential stage of the model development since parameters such as the time step can considerably affect the reliability of the model. The chosen convergence criterion is based

The simulation run for these tests departs from a uniform temperature of 15 °C. The oven and fridge are kept 'on' throughout the calculation and the radiator is functioning to insure a room temperature of 20 °C. No coating is present such that a standard emissivity of 0.9 is applied to all surfaces.

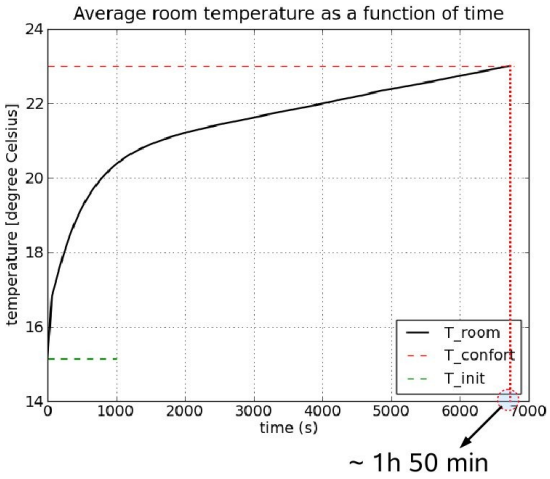

Figure 3. Temperature rise in the room

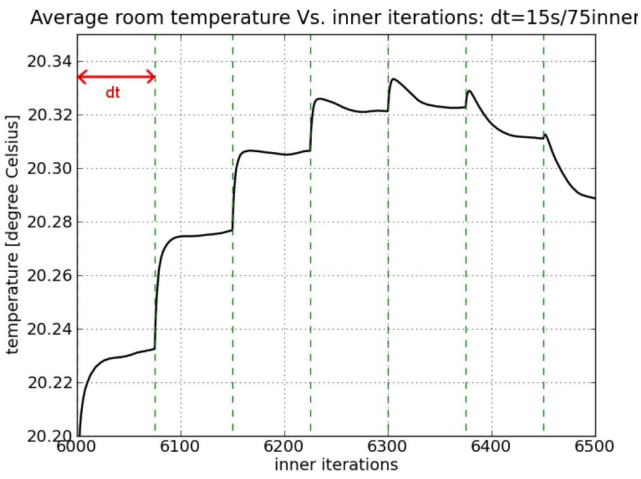

Figure 4. Time step dependency study

The time step is to be adjusted along with the number of inner-iterations in order to allow the flow to converge in between each time step. In the case of low speed flows driven by natural convection, the residuals can be misleading. A safer alternative is to look at how the flow quantities converge. On figure 4, the average room temperature chosen as convergence criterion is plotted as a function of the inner iteration number for a time step of 15 seconds and 75 inner iterations. It can be seen that this combination of values is sufficient to allow the quantity to stabilize. This behavior allows for slightly fewer inner iterations, reduced down to 60 for a fixed time step of 15 seconds.

4. Implementation of the CFD simulation

4.1. Scenario

A standard scenario is designed to be as representative as possible of the typical usage of a kitchen. The physical time covered by the simulation is fixed to 3 hours so that a result can be obtained in about 12 hours on 32 processors. To remain realistic, the fridge is kept 'on' throughout the run and the oven is switched on after 90 minutes and functions for 45 minutes. As for the radiator, it follows a cyclic behavior in winter to maintain a comfort temperature of 20 °C around the thermostat region. The reference temperature T_{ref} is averaged within a control volume [0.6x0.6x0.3 m] located close to the middle of the internal wall (x-) at 1 meter high.

4.2. Simulation cases

The emissivity is the only parameter investigated here and moreover, the coating is applied to the interior wall surfaces and outer casings of the appliances. Firstly, the ground was excluded from the walls of interest and the remaining surfaces were regrouped in a logical way so as to focus on the most informative configurations. This approach leaves us with 4 groups of surfaces, namely the interior walls (x-, y±), the exterior wall (x+), the ceiling (z+) and the outer casings of the oven and fridge. Consequently there are 4 inputs that remain, corresponding to the emissivity values of each of these groups of surface, namely $\varepsilon_{m,int}$, ε_{x+}, ε_{z+} and ε_{f-f} respectively, which for simplicity can take only two values representative of the presence or not of the coating. One of the objectives being to exploit the entire domain, a standard value of 0.9 is chosen in the absence of coating and a very low-emissivity value of 0.1 otherwise. All other surfaces are kept at 0.9. All 16 possible combinations listed in table 3 are simulated. The case 1 for which all surfaces are standard will be taken as reference. From cases 2 to 5, the effect of only one input is considered since the coating is applied to a single group of surfaces. A combination of surfaces are coated from cases 6 to 15, while all of them are in the last case 16. This series of configurations will allow to first isolate the influence of each input separately and then consider the way these interact with each other. In summer conditions however, the runs were limited to the most instructive cases 1-5 and 16., denoted s1-s5 and s16 respectively.

Table 3. Simulation cases

Case	1	2	3	4	5	6	7	8	9	10	11	12	13	14	15	16
$\varepsilon_{m,int}$	0.9	0.1	0.9	0.9	0.9	0.1	0.1	0.1	0.9	0.9	0.9	0.1	0.1	0.9	0.1	0.1
ε_{z+}	0.9	0.9	0.1	0.9	0.9	0.1	0.9	0.9	0.1	0.9	0.1	0.1	0.1	0.1	0.9	0.1
ε_{x+}	0.9	0.9	0.9	0.1	0.9	0.9	0.1	0.9	0.1	0.1	0.9	0.1	0.9	0.1	0.1	0.1
ε_{f-f}	0.9	0.9	0.9	0.9	0.1	0.9	0.9	0.1	0.9	0.1	0.1	0.9	0.1	0.1	0.1	0.1

4.3. Initial state

A common initialization technique is adopted to begin the transient simulations from a realistic state. Indeed, it is critical to start with a room already in regime considering its inertia and particularly of the walls. All as important, thermal stratification caused by thermal gradients should be present. To best

match these conditions, steady calculations were run with all of the equipments switched-off, and the average room temperature was forced to approach an initial value T_{init} of 15 °C. This value was imposed through a volume source defined as: $Q_{source,i} = \alpha . (T_{init} - T_{ref,i})$, where $Q_{source,i}$ is the amount of heat injected at iteration i. This source forces the reference temperature to strive towards the desired temperature. Figures 5 and 6 (case 1) illustrate the thermal stratification present in the room and the wall temperature distributions respectively.

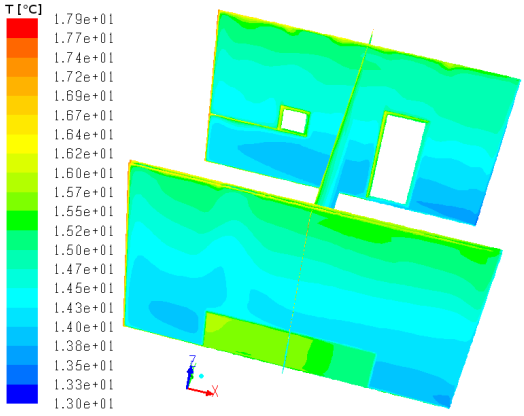

Figure 5. Initial stratification

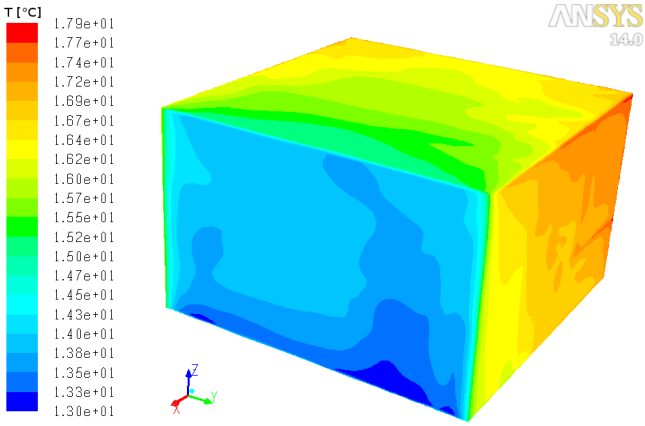

Figure 6. Wall temperature gradients

5. Parametric study

5.1. Influence of the coating in winter conditions

Interpreting the results is relatively intuitive since the analysis is based on the radiator's power contribution, closely related to heat consumption. Firstly, the individual effect of the different groups of surfaces shown on figure 7 (cases 2 to 5) are investigated before looking into the more complex configurations. In the reference case 1, for which none of the surfaces are coated, the mean power contribution is of 315 W over the 3 hour run. The exterior wall increases the required contribution by about 5 % while the appliances have the opposite effect. This positive influence is amplified in the case of the ceiling (~12%) and furthermore for the interior walls (~24%). Although limited, the gain obtained thanks to the appliances can be attributed to the temperature rise experienced by the oven's outer casing which heats up even more its environment. However, the gain does not exceed 4.7 % due to a limited exchange surface and operating period (a quarter of the simulation time).

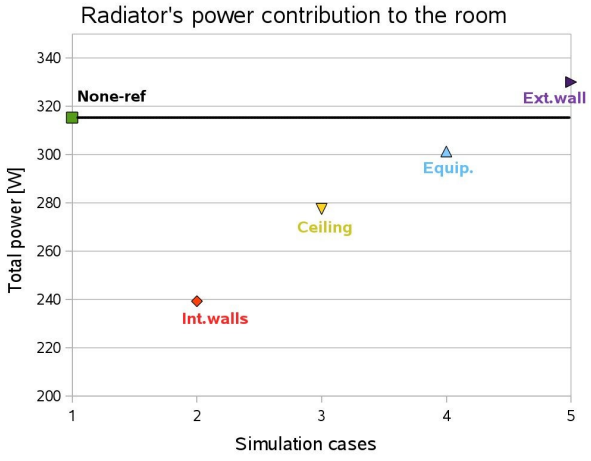

Figure 7. Radiator's contributions

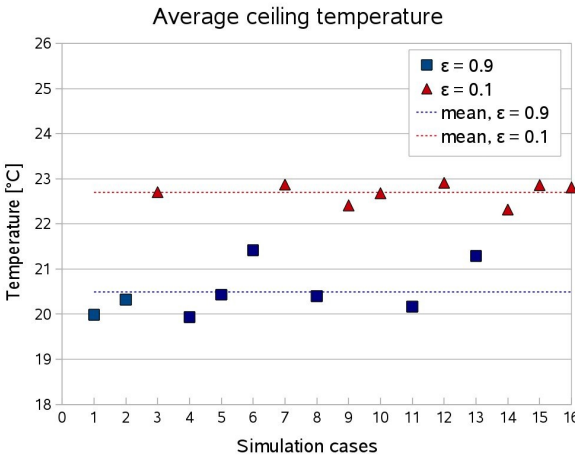

Figure 8. Temperature changes (z+)

When applied to the exterior wall, the coating causes a temperature drop of 2.5 °C, its interior surface decreasing from 16.8 down to 14.3 °C in average as can be seen on figure 9. Naturally, this impacts on the room, with the ambient air further cooled down by the surface, as shown by the CHTC values represented on figure 10, reinforced by more than 60 %. To conclude, these results indicate that the colder the surface compared to the room, the larger the energy loss as the coating amplifies the temperature difference.

At the contrary, the ceiling is by nature warmer than the room (T_c ~20 °C) as it is in direct contact with the warmer air, driven upwards by natural convection. In agreement with previous studies [11, 12], results indicate that a significant reduction in total heat flux can be achieved with a low emissivity ceiling surface. The coating amplifies these effects with a temperature that increases from 20.5 °C to 22.7 °C as shown by figure 8, reducing the radiator's contribution by 12 %.

Finally, although the impact of the interior walls is the strongest with a 24 % energy gain, the role played by these surfaces is difficult to interpret due to the multiple exchange surfaces. Nevertheless some of these interactions clearly stand out. Referring to figure 11, the temperature drops experienced by wall (y+), encircled in black, coincide to everyone of the coated configurations. Indeed, the wall is being less warmed-up by the exchanger and radiator plates it directly faces. Considering now wall (x-) opposite to the colder wall (x+) in contact with the exterior, these same cases correspond to temperature rises as the coating causes the opposite effect. The temperature variations observed by wall (y-) are harder to relate because of surface interactions. Due to these and the very small temperature differences, the influence of the interior walls appears more complex than for the other surface groups, but results indicate that in these conditions the coating is very beneficial.

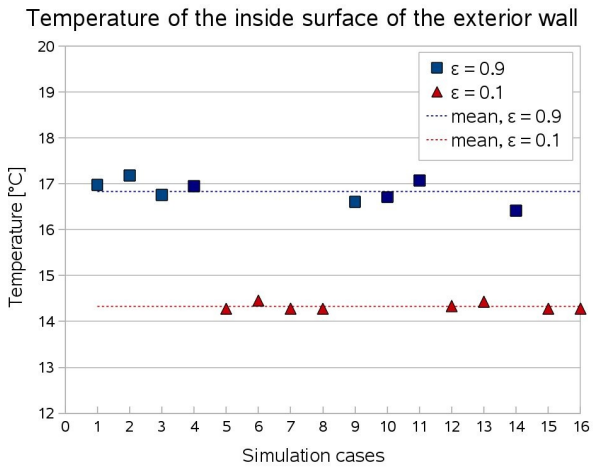

Figure 9. Temperature changes (x+)

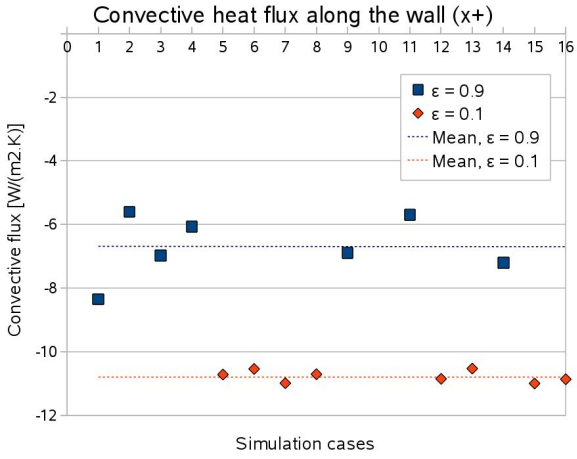

Figure 10. Convective changes (x+)

To complete this analysis, the results provided by the remaining simulations (6-16) are analyzed, in which the coating is not only applied to a single group of surfaces but to a combination. All results, reported on figure 12, are categorized in four classes according to the relative difference (/case 1) in the radiator's power contribution: losses [0% ; +5%], weak gains [0% ; -10 %], medium gains [-10 % ; -22 %] and strong gains [-22 % ; -30 %].

In the first category “losses”, both cases 5 and 8 have the coating applied to the exterior wall (x+), which has a negative influence as seen previously. In case 8, coating the appliances in addition has a limited effect at room scale. As for 'simple' case 4 where the oven and fridge are coated, in case 7 “weak gains” result from losses induced by the coated exterior wall (x+) compensated by the positive influence of the coated ceiling.

"Medium gains" are associated to 'simple' case 3 for which the coating is applied to the ceiling. Case 10 provides similar gains with in addition coated appliances, while case 15 includes 3 groups, coating also the exterior wall (x+). Also in this category are combinations of exterior wall (x+) who's losses are compensated by the interior walls, with and without appliances (cases 6 and 13 respectively).

For the best configurations, the energy gain exceeds 22 % thanks to the coated interior walls. This last group of surfaces dominates in any case, except when the coating is also applied to the exterior wall (x+) which slightly diminishes the gains down to medium. To conclude, the coating behaves logically in these combined cases since generally the results correspond to a superposition of 'simple' cases that conserve their own positive or negative influences.

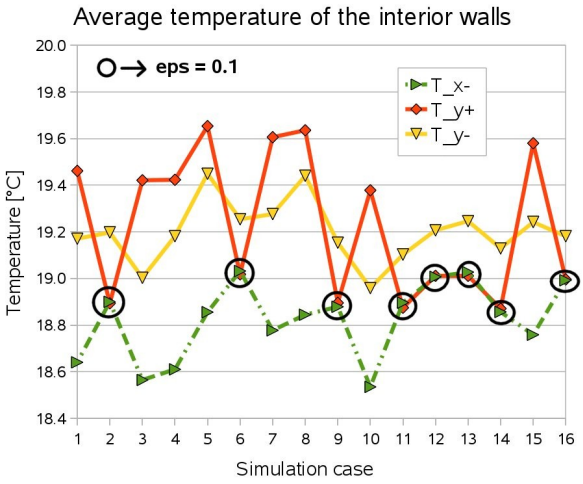

Figure 11. Wall temperature changes

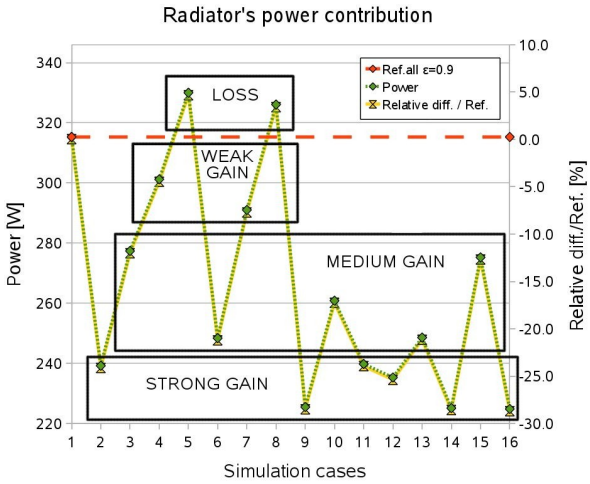

Figure 12. Simulation classification

To finalize this comparison, we should mention that there are several factors that determine comfort of occupants within a room. There is not only ambient air temperature but also humidity, radiation, air movement, intrinsic clothing and level of activity. However, in the frame of this project, measurable parameters are air temperature and wall temperatures. The 'felt' temperature can be simplified down to an average value of air and wall temperature. By comparing the time average values obtained in cases 1 and 16, the difference is only of 0.2 °C. Consequently, we may assume that the difference in terms of additional energy required to reach the exact same 'felt' temperature would be negligible.

5.2. Room comfort in summer conditions

In summer conditions, the analysis of the coating's effect at room level is conducted based on the room temperature differences. The time variations throughout the simulation are compared on figure 13.

These distributions indicate that the coating does not lead to any improvement compared to the standard case 1 since the room temperature increases. Nevertheless, in the most disadvantageous cases this rise is limited to about 1.3 °C when the oven is 'on', and 0.6 °C otherwise. Once again, each case can be classified into 3 different categories according to the temperature increase observed at room level: negligible [0 °C ; 0.2 °C] when applied to appliances and exterior wall, very weak [0.2 °C ; 0.4 °C] for the ceiling and weak [0.4 °C ; 1.3 °C] when the interior walls are coated.

To conclude, the coating does not bring any gain in the summer but it is important to note that the comfort conditions are very weakly affected by its presence since over-heating (> 25 °C when oven off) is avoided. Consequently, it appears perfectly reasonable to apply permanently the coating to benefit from the energy savings achieved in winter, provided the surfaces to coat are carefully chosen.

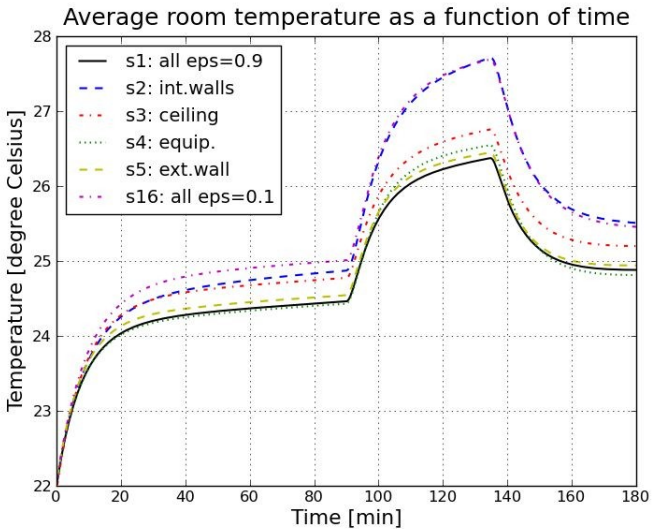

Figure 13. Room temperature distributions in summer

6. Conclusions

To conclude, this study has shown that a low-emissivity coating is able to considerably reduce the heating consumption of the room. A high degree of reliability was insured by scrupulously implementing the cavity model for it to be as representative as possible of the modeled kitchen. The boundary conditions were imposed according to standards and parameters tuned following common sense and in agreement with published studies. An important effort was also dedicated to choosing the models and simulation parameters such as the time step. Based on this simulation model, the parametric study was implemented to satisfy the problematic as efficiently as possible. The calculation effort was reduced by limiting the potential areas of application of the coating to the most relevant.

The results demonstrate that the coating can have a significant impact in certain configurations, identified following a case by case analysis. For instance, it is advantageous to coat the surfaces that are warmer than the room such as the ceiling. Indeed, the convective heat exchange is reinforced, allowing to fully benefit from the temperature gradient to heat up the ambiant air which results in a reduced number of radiator cycles. At the contrary, applying the coating to colder surfaces such as the exterior wall in winter conditions, can lead to the opposite effect. It is thanks to their important exchange surface that the interior walls have the strongest impact, with close to 25 % less contribution needed from the radiator. However, in summer these cause the strongest temperature rise (~1 °C) although in any case this same effect is obtained, but avoiding any substantial overheating. It is therefore possible to fully benefit from the energy gains achieved in winter.

Although the aim was to focus here on heating consumption, these results could also be exploited in the future to investigate the influence of the low emissivity coating on the losses experienced by the oven and fridge. An important reduction is foreseen which could be particularly attractive to appliance manufacturers.

7. References

[1] ANSYS Inc. 2009 ANSYS Fluent 13.0 Documentation
[2] ISO 13790: Energy performance of buildings – Calculation of energy use for space heating and cooling, 2008
[3] Ashrae 1998 ASHRAE Handbook, 1998 Refriferation Volume (Atlanta: Inch-Pound Edition)

[4] Alfonso C, Matos J 2006 The effect of radiation shields around the air condenser and compressor of a refrigerator on the temperature distribution inside it *International Journal of Refrigeration* **29** 1144-1151
[5] Illes B 2010 Distribution of the heat transfer coefficient in convection reflow oven *Applied Thermal Engineering* **30** 1523-1530.
[6] Carson J K, Willix J, North M F 2006 Measurements of heat transfer coefficients within convection ovens *Journal of Food Engineering* **72** 293-301
[7] Laguerre O, Benamara S, Flick D 2010 Numerical simulation of simultaneous heat and moisture transfer in a domestic refrigerator *International Journal of Refrigeration* **33** 1425-1433
[8] Laguerre O, Benamara S, Flick D 2005 Experimental study of heat transfer by natural convection in a closed cavity: application in a domestic refrigerator *Journal of Food Engineering* **70** 523-537
[9] Laguerre O, Benamara S, Moureh J, Flick D 2007 Numerical simulation of air flow and heat tranfer in domestic refrigerators *Journal of Food Engineering* **81** 144-156
[10] Photovoltaic Geographical Information System, Joint Research Centre, European Commission (http://re.jrc.ec.europa.eu/pvgis/)
[11] Joudi M A, Ronnelid M, Sveding H, Wackelgard E 2011 Energy Efficient Buildings with Functional Steel Cladding *World Renewable Energy Congress 2011, Sweden.*
[12] Daoud A, Galanis N, Bellache O 2008 Calculation of refrigeration loads by convection, radiation and condensation in ice rinks using transient 3D zonal model *Applied Termal Engineering* **28** 1782-1790.